

Phonon transport in Na₂He at high pressure from a first-principles study

San-Dong Guo and Ai-Xia Zhang

¹*School of Physics, China University of Mining and Technology, Xuzhou 221116, Jiangsu, China*

Phonon transport of recently-fabricated Na₂He at high pressure is investigated from a combination of first-principles calculations and the linearized phonon Boltzmann equation within the single-mode relaxation time approximation (RTA). The calculated room-temperature lattice thermal conductivity is 149.19 Wm⁻¹K⁻¹, which is very close to one of Si. It is found that low-frequency optical modes comprise 16% of the lattice thermal conductivity, while high-frequency optical modes have negligible contribution. The high lattice thermal conductivity is due to large group velocities, small Grüneisen parameters, and long phonon lifetimes. The size effects on lattice thermal conductivity are considered by cumulative thermal conductivity with respect to phonon mean free path(MFP). To significantly reduce the lattice thermal conductivity, the characteristic length smaller than 100 nm is required, and can reach a decrease of 36%. These results may be useful to understand thermal transport processes that occur inside giant planets.

PACS numbers: 72.15.Jf, 71.20.-b, 71.70.Ej, 79.10.-n

Keywords: Lattice thermal conductivity; Group velocities; phonon lifetimes

Email:guosd@cumt.edu.cn

I. INTRODUCTION

Helium is chemically inert, and it is difficult to form thermodynamically stable compounds. Recently, a stable high-pressure phase Na₂He with a fluorite-type structure is discovered in experiment, which is stable from 113 GPa up to at least 1000 GPa¹. By the first-principles calculations, it is predicted that Na₂He displays insulating properties, and the energy band gap increases with increasing pressure. It is interesting and necessary to investigate other physical properties of Na₂He, such as heat transport. In semiconductors, the lattice part usually carries the majority of heat around room temperature and higher, while electronic part has negligible contributions to the thermal conductivity. The lattice thermal conductivity is mainly an anharmonic phenomenon. Recently, the first-principles calculations can predict anharmonic force constants quantitatively, and then provide accurate information about the intrinsic phonon-phonon scattering based on the solution of the phonon Boltzmann transport equation²⁻¹¹. Further, the lattice thermal conductivity can be well reproduced, being in agreement with experimental results using no adjustable parameters.

Here, we investigate phonon transport of Na₂He with the single-mode RTA of the linearized phonon Boltzmann equation. The lattice thermal conductivity with respect to temperature is calculated, and the room-temperature value is 149.19 Wm⁻¹K⁻¹, which is very close to 155 Wm⁻¹K⁻¹ of Si¹². The small Grüneisen parameters of Na₂He indicates a weak anharmonicity, leading to the high thermal conductivity. The large group velocities and long phonon lifetimes can also explain high thermal conductivity. Moreover, we find that the low-frequency optical modes contribute observably to the total thermal conductivity, while high-frequency optical phonons can be neglected. To measure phonon MFP, the thermal conductivity spectroscopy technique has been developed¹³, which can measure MFP distributions over a wide range of length scales. Therefore, the cumulative lattice ther-

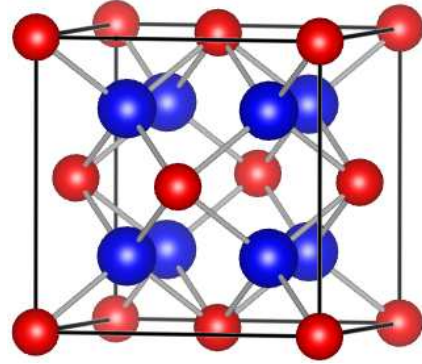


FIG. 1. An illustration of Na₂He crystal structure. The large blue balls represent Na atoms, and small red balls for He atoms.

mal conductivity with respect to phonon MFP is calculated, which can be used to study size effects in heat conduction.

The rest of the paper is organized as follows. In the next section, we shall give our computational details. In the third section, we shall present phonon transport of Na₂He. Finally, we shall give our discussions and conclusions in the fourth section.

II. COMPUTATIONAL DETAIL

The lattice thermal conductivity of Na₂He is performed with the single mode RTA and linearized phonon Boltzmann equation, which can be achieved by using Phono3py+VASP codes^{5,15-17}. For the first-principles calculations, the framework of the all-electron projector augmented wave (PAW) method within the density functional theory¹⁴ is employed, as implemented in the package VASP¹⁵⁻¹⁷. The generalized gradient approximation (GGA) of Perdew-Burke-Ernzerhof (PBE) is adopted as the exchange-correlation functional¹⁸. A plane-wave ba-

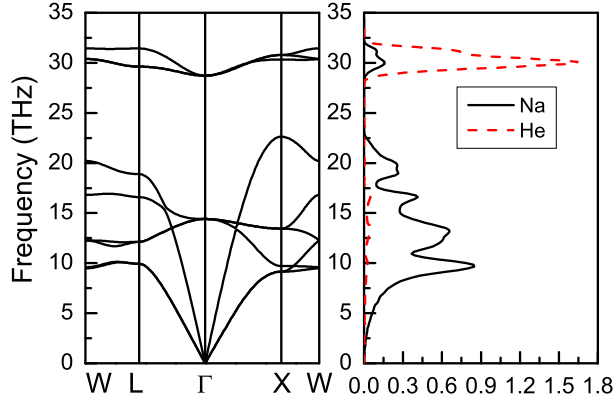


FIG. 2. Phonon band structures and partial DOS of Na_2He .

sis set is used with kinetic energy cutoff of 1000 eV. The second order harmonic and third order anharmonic interatomic force constants (IFC) are calculated by using a $3 \times 3 \times 3$ supercell and a $2 \times 2 \times 2$ supercell, respectively. Using the harmonic IFCs, the group velocity and specific heat can be attained by phonon dispersion relation, and phonon dispersion determines the allowed three-phonon scattering processes. The third-order anharmonic IFCs can determine the phonon lifetimes, which can be attained by calculating the three-phonon scattering rate. To compute lattice thermal conductivities, the reciprocal spaces of the primitive cells are sampled using the $20 \times 20 \times 20$ meshes.

III. MAIN CALCULATED RESULTS AND ANALYSIS

The Na_2He has a fluorite-type structure with space group $Fm\bar{3}m$ at 300 GPa¹. The Na and He atoms occupy the Wyckoff position 8c (0.25,0.25,0.25) and 4a (0,0,0), respectively. The schematic crystal structure is shown in Figure 1. The experimental lattice parameter $a=3.95$ Å is employed to investigate its phonon transport. Based on harmonic IFCs, the phonon dispersions are calculated along high-symmetry pathes, which is shown in Figure 2, together with partial density of states (DOS). The unit cell of Na_2He contains three atoms, resulting in 3 acoustic and 6 optical phonon branches in the phonon spectra. According to Figure 2, a gap of 6.09 THz can be observed, which separates three high-frequency optical modes from the low-frequency modes. The high-frequency optical modes are mainly from He vibrations, while the acoustic and low-frequency optical modes of phonon dispersions mainly is due to the vibrations of the Na atoms. The low-frequency optical modes have larger dispersion than high-frequency ones, indicating that low-frequency ones have relatively large group velocities.

Figure 3 shows the lattice thermal conductivity of Na_2He as a function of temperature, the accumulated lattice thermal conductivity (300 K) along with

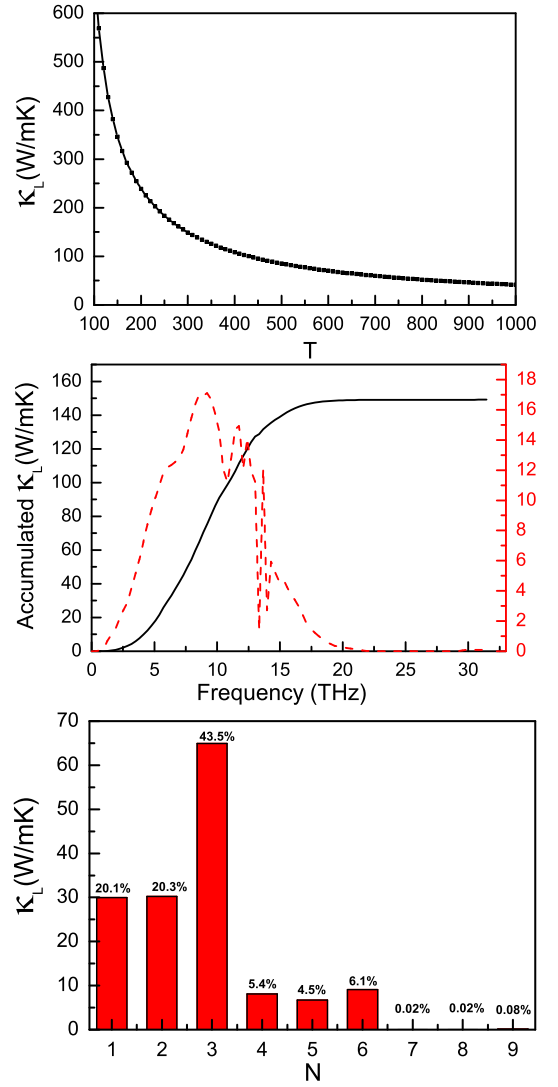


FIG. 3. (Color online) Top: the lattice thermal conductivity of Na_2He as a function of temperature; Middle: the accumulated lattice thermal conductivity (300 K), and the derivatives; Bottom: phonon modes contributions toward total lattice thermal conductivity (300 K).

the derivatives, and phonon modes contributions toward total lattice thermal conductivity (300 K). The room-temperature lattice thermal conductivity is $149.19 \text{ Wm}^{-1}\text{K}^{-1}$, and the lattice thermal conductivity nearly meets the $1/T$ relation at high temperature (above room-temperature). As shown in Figure 3(Middle), the acoustic phonon branches below the 13.34 THz dominate lattice thermal conductivity, and the peak of the derivatives drops rapidly at 13.34 THz. The remaining contribution is almost from low-frequency optical modes, while the high-frequency optical modes show a neglectful contribution to lattice thermal conductivity, also found in other semiconductors¹². Further, the relative contributions of every acoustic and optical phonon mode to the total lattice thermal conductivity are examined. The two trans-

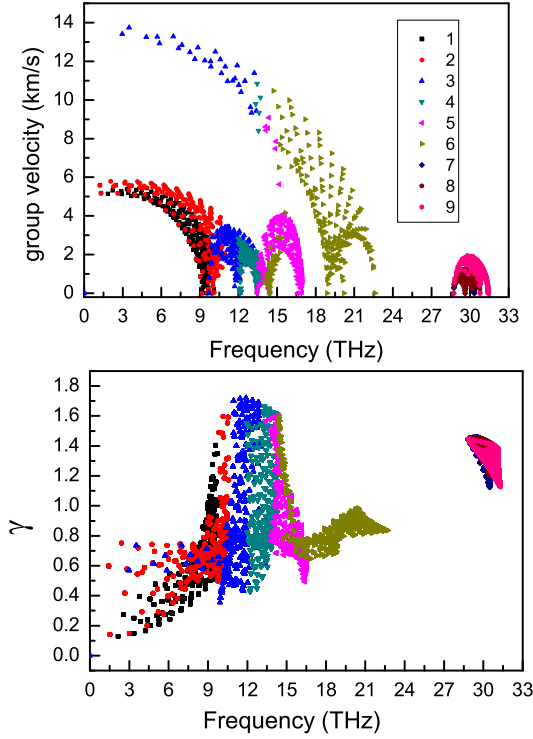


FIG. 4. (Color online) The phonon mode group velocities (Top) and mode Grüneisen parameters (Bottom) of Na_2He in the first Brillouin zone.

verse acoustic (TA) branches have almost the same contributions of about 20%, while the longitudinal acoustic (LA) branch has the largest contributions, as high as 44%, which is twice the contribution of TA branch. The low-frequency optical branches provide a contribution of about 16%, while high-frequency ones only 0.12%.

The phonon mode group velocities and mode Grüneisen parameters (γ) of Na_2He in the first Brillouin zone are plotted in Figure 4. It is found that the group velocity of LA branch is larger than ones of TA branches at low-frequency region, and the largest group velocity for LA and TA branches near Γ point is 13.74 km s^{-1} and 5.79 km s^{-1} , respectively. It is also clearly seen that the third optical branch shows relatively large group velocities due to larger dispersion. Mode Grüneisen parameters are calculated from third order anharmonic IFCs, and they all are positive throughout the Brillouin zone. The mode Grüneisen parameters can reflect the strength of anharmonic interactions, and larger γ induces lower lattice thermal conductivity due to strong anharmonicity. The high value region of mode Grüneisen parameters focuses primarily between 8 THz and 16 THz, and the maxima is 1.72. The mode Grüneisen parameters of Na_2He are smaller than ones of BiCuOSe ¹⁹ and PbTe ²⁰ with low high lattice thermal conductivities as representative thermoelectric materials. The average mode Grüneisen parameters is 1.02, which means weak anharmonicity, leading to high lattice thermal conductivity.

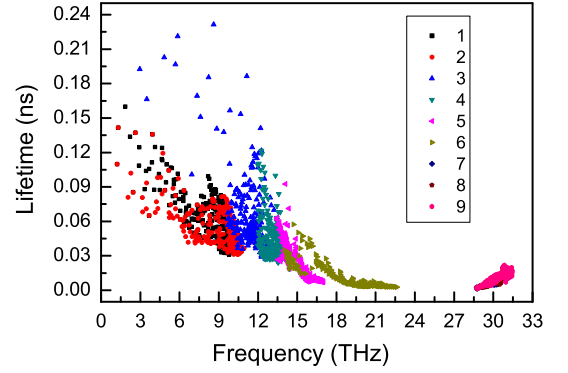


FIG. 5. Phonon lifetimes of Na_2He at room temperature.

The three-phonon scattering rate can be attained by third-order anharmonic IFCs, and phonon lifetimes can be calculated. Phonon lifetimes of Na_2He at room temperature are shown in Figure 5, which are reciprocal of the phonon linewidth. The lattice thermal conductivity and phonon lifetimes are merely proportional to each other in the single-mode relaxation time method⁵. The lifetimes of most acoustic modes are between 40 ps and 90 ps, and the ones of low-frequency optical modes decrease with increasing frequency. The first optical branch of them has long lifetimes, being well-matched with ones of acoustic modes. They lie in 2 ps to 22 ps for high-frequency optical modes. The distribution of phonon lifetimes can mainly explain the relative contributions of every acoustic and optical phonon mode to the total lattice thermal conductivity.

The cumulative lattice thermal conductivity along with the derivatives with respect to phonon MFP is shown in Figure 6 at room temperature, which provides information about the contributions of phonons with different MFP to the total thermal conductivity. The phonon MFP is also useful to understand and engineer size effects on lattice thermal conductivity. The total accumulation increases with MFP increasing, and the accumulation gradually approaches plateau after MFP reaches 440 nm. Phonons with MFP smaller than 100 nm contribute around 64% to the lattice thermal conductivity.

IV. DISCUSSIONS AND CONCLUSION

It is interesting to compare phonon transport of Na_2He with other semiconductor materials, such as Si and PbTe . The frequency range of acoustic modes between Na_2He and Si ¹² is almost the same, and their phonon lifetimes have the same order of magnitude⁶. Therefore, the room-temperature lattice thermal conductivity of Na_2He ($149.19 \text{ W m}^{-1} \text{ K}^{-1}$) is very close to $155 \text{ W m}^{-1} \text{ K}^{-1}$ of Si. The acoustic frequency range of Na_2He is very wider than one of PbTe ⁷, which leads to larger group velocities. The phonon lifetimes of PbTe are very shorter than

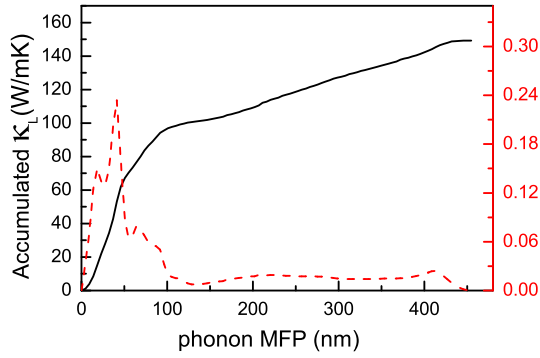


FIG. 6. (Color online) Cumulative lattice thermal conductivity of Na_2He with respect to phonon mean free path at room temperature.

ones of Na_2He . So, the lattice thermal conductivity ($1.9 \text{ Wm}^{-1}\text{K}^{-1}$) of PbTe at 300 K is very lower than one of Na_2He . The similarity between Na_2He and PbTe is that the contributions of optical phonons to lattice thermal conductivity remain very large, 16% for Na_2He and 22% for PbTe at room temperature. However, for Si, the optical branches comprise only 5% of the lattice thermal conductivity^{21–23}. The difference among them is size effects on lattice thermal conductivity, which can be described by cumulative lattice thermal conductivity as a

function of MFP. MFPs smaller than 10 nm contribute to around 90% of the lattice thermal conductivity for PbTe ⁷. Phonons with MFP smaller than 100 nm comprise around 64% of the lattice thermal conductivity for Na_2He . MFPs smaller than 1000 nm contribute to almost half of the total thermal conductivity for Si⁶.

In summary, the intrinsic lattice thermal conductivity of Na_2He is calculated based mainly on the reliable first-principle calculations and Boltzmann transport theory. The room-temperature lattice thermal conductivity is found to be $149.19 \text{ Wm}^{-1}\text{K}^{-1}$. The acoustic and low-frequency optical branches provide nearly 100% contribution to total lattice thermal conductivity. The high lattice thermal conductivity is due to weak anharmonicity and high group velocities. In addition, the size effects on thermal conductivity are also studied by cumulative lattice thermal conductivity with respect to MFP. The present work can encourage further efforts to investigate other chemical and physical properties of Na_2He .

ACKNOWLEDGMENTS

This work is supported by the National Natural Science Foundation of China (Grant No. 11404391). We are grateful to the Advanced Analysis and Computation Center of CUMT for the award of CPU hours to accomplish this work.

- ¹ D. Xiao et al., Nat. Chem. (2017).
<http://dx.doi.org/10.1038/nchem.2716>
- ² L. Chaput, Phys. Rev. Lett. **110**, 265506 (2013).
- ³ A. Ward, D. A. Broido, D. A. Stewart and G. Deinzer, Phys. Rev. B **80**, 125203 (2009).
- ⁴ A. Ward and D. A. Broido, Phys. Rev. B **81**, 085205 (2010).
- ⁵ A. Togo, L. Chaput and I. Tanaka, Phys. Rev. B **91**, 094306 (2015).
- ⁶ K. Esfarjani, G. Chen and H. T. Stokes, Phys. Rev. B **84**, 085204 (2011).
- ⁷ Z. Tian, J. Garg, K. Esfarjani, T. Shiga, J. Shiomi and G. Chen, Phys. Rev. B **85**, 184303 (2012).
- ⁸ T. Shiga, J. Shiomi, J. Ma, O. Delaire, T. Radzynski, A. Lusakowski, K. Esfarjani and G. Chen, Phys. Rev. B **85**, 155203 (2012).
- ⁹ W. Li, J. Carrete, N. A. Katcho and N. Mingo, Comput. Phys. Commun. **185**, 1747 (2014).
- ¹⁰ L. Lindsay, D. A. Broido and T. L. Reinecke, Phys. Rev. Lett. **109**, 095901 (2012).
- ¹¹ L. Lindsay, D. A. Broido and T. L. Reinecke, Phys. Rev. Lett. **111**, 025901 (2013).
- ¹² L. Lindsay, D. A. Broido and T. L. Reinecke, Phys. Rev. B **87**, 165201 (2013).
- ¹³ A. J. Minnich, J. A. Johnson, A. J. Schmidt, K. Esfarjani, M. S. Dresselhaus, K. A. Nelson and G. Chen, Phys. Rev. Lett. **107**, 095901 (2011).
- ¹⁴ P. Hohenberg and W. Kohn, Phys. Rev. **136**, B864 (1964); W. Kohn and L. J. Sham, Phys. Rev. **140**, A1133 (1965).
- ¹⁵ G. Kresse, J. Non-Cryst. Solids **193**, 222 (1995).
- ¹⁶ G. Kresse and J. Furthmüller, Comput. Mater. Sci. **6**, **15** (1996).
- ¹⁷ G. Kresse and D. Joubert, Phys. Rev. B **59**, 1758 (1999).
- ¹⁸ J. P. Perdew, K. Burke and M. Ernzerhof, Phys. Rev. Lett. **77**, 3865 (1996).
- ¹⁹ H. Z. Shao, X. J. Tan, G. Q. Liu, J. Jiang and H. C. Jiang, Sci. Rep. **6**, 21035 (2016).
- ²⁰ Y. Zhang, X. Z. Ke, C. F. Chen, J. Yang and P. R. C. Kent, Phys. Rev. B **80**, 024304 (2009).
- ²¹ A. S. Henry and G. Chen, J. Comput. Theor. Nanosci. **5**, 141 (2008).
- ²² D. A. Broido, M. Malorny, G. Birner, N. Mingo, and D. A. Stewart, Appl. Phys. Lett. **91**, 231922 (2007).
- ²³ D. P. Sellan, J. E. Turney, A. J. H. McGaughey, and C. H. Amon, J Appl. Phys. **108**, 113524 (2010).